Experimental investigation of 50 MPa reinforced concrete slabs subjected to blast loading

Investigación experimental de losas de concreto armado de 50 MPa sometidas a efecto de explosión

Fausto Mendonça[1], Girum Urgessa[2], and José Rocco[3]

ABSTRACT

This paper presents the results from blast tests conducted on four 50 MPa concrete slabs with reinforcement ratios of 0,175% and 0,37%. Two of the slabs were retrofitted with 50 mm thick foam in order to investigate the potential of using the foam as a strengthening option. The slabs were simply supported on two sides. Non-confined PBX (Plastic bonded explosive) was molded with the form of a cylinder measuring 20 cm in height and 10,5 cm in diameter. The explosive was detonated at 2 m stand-off distance. The equivalent TNT mass of the explosive ranges from 2,58 to 2,72 kg for the four tests. Accelerometers, displacement and pressure gages were used to measure blast wave parameters and global response of the slabs. A high-speed digital camera in conjunction with a rugged notebook recorded images. Qualitative and quantitative results are included. Slabs retrofitted with foam showed a different pressure pattern as recorded by the sensors and resulted in higher displacement, acceleration and linear momentum.

Keywords: Blast effect, retrofitting, concrete slabs, non-confined explosive.

RESUMEN

Este documento presenta los resultados de una prueba experimental de efecto de explosiones y de instrumentación desde el subconjunto de cuatro losas de concreto de 50 MPa con ratios de refuerzo del 0,175% y 0,37%. Dos de las losas han sido protegidas con una espuma de poli estireno expandido con 50 mm de espesor para poder comprobar la capacidad que tiene la espuma de modificar la respuesta a la explosión. Las losas se apoyaron en dos lados. El explosivo plástico PBX (por las siglas en inglés de *plastic bonded explosive*) no confinado fue moldeado en forma de cilindro teniendo 20 cm de alto y 10,5 cm de diámetro. El explosivo fue detonado a 2 metros de distancia. La masa de equivalente TNT de los explosivos varía entre 2,58-2,72 kg. Acelerómetros, medidores de desplazamientos y sensores de presión fueran utilizados para medir los parámetros de la onda de choque y la respuesta global de las losas. Una cámara digital de alta velocidad conectada a una computadora portátil robusta grabó las imágenes. Se incluyen datos resultados cualitativos y cuantitativos. Las losas con protección de espuma variaron el patrón de presión registrados por los sensores y resultó en un mayor desplazamiento, aceleración y el momento lineal.

Palabras clave: Efecto de explosión, protección, losas de concreto, explosivo no confinado.

Introduction

There is a growing interest in understanding the response of reinforced concrete slabs that are subjected to the effects of explosive (Castedo *et al.*, 2015; Li *et al.*, 2016). In addition, finding and characterizing retrofit mechanisms to mitigate the effects of blast continues to be of interest to private and government entities (Urgessa & Maji, 2010). One cheap retrofitting scheme is to use a foam with a long yield plateau for absorbing blast energy (Mendonça

et al., 2017; Petel *et al.*, 2013). A few studies have shown that foam retrofits increased the imparted impulse on the protected structures exacerbating total damage based on numerical simulation (Lee & O'Toole, 2004; Mendonça *et al.*, 2017; Mullin & O'Toole, 2004). However, these studies lack direct comparison or correlations using field tests.

To address the gaps in the literature, multiple blast tests were conducted on reinforced concrete slabs measuring 1,0 m × 1,0 m in plan and 0,08 m in thickness, at the Science and Technology Aerospace Department (DCTA) stand site in São José dos Campos, São Paulo, Brazil. This paper presents the

[1] Civil Engineer, Rio de Janeiro State University, Brazil. M.Sc., University of Brasília, Brazil. Ph.D., Technological Institute of Aeronautics, Brazil. E-mail: fausto@ita.br.

[2] Civil Engineer, Addis Abada University, Ethiopia. M.Sc., University of New Mexico, USA. Ph.D., University of New Mexico, USA. Affiliation: Associate Professor, George Mason University, USA. E-mail: gurgessa@gmu.edu.

[3] Chemical Engineer, Faculty of Industrial Engineering, Brazil. M.Sc., Technological Institute of Aeronautics, Brazil. Ph.D., Technological Institute of Aeronautics, Brazil. Affiliation: Associate Professor, Technological Institute of Aeronautics, Brazil. E-mail: friz@ita.br.

description of the experimental test set-up, instrumentation and results from a sub-set of the blast tests conducted on four 50 MPa concrete slabs with reinforcement ratios of 0,175% in one direction and 0,37% in the perpendicular direction. In addition, two of the four slabs were retrofitted with 50 mm thick expanded polystyrene foam (EPS) on the upper surface of the slab, to determine whether the foam has the capacity to reduce or exacerbate the blast response of the slab. Figure 1 shows the setup of the full-scale test with a stand-off distance (R) of 2 m.
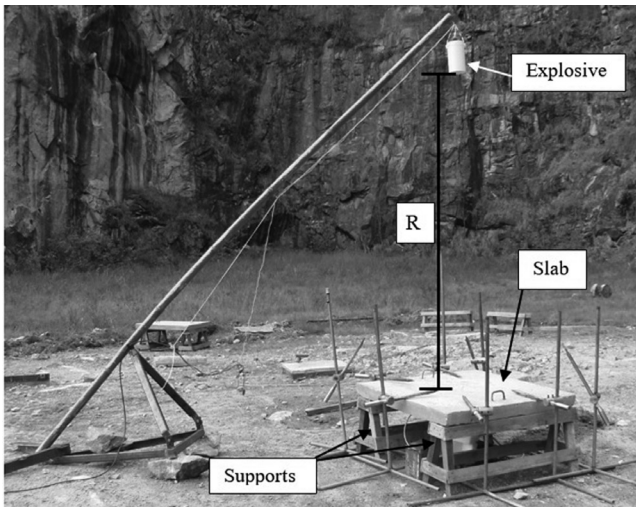

Figure 1. Test setup.
Source: Authors

Experimental Setup

The explosive

The plastic bonded explosive used in this experiment contains 2,70 kg of equivalent TNT mass. The explosive was PBX (Plastic-bonded explosive) with 80% of HMX (High Melting point Explosive) and 20% of binder. More details about the explosive can be found in Kirchhof *et al.* (2016). The body of the explosive was cylindrical in shape measuring 20 cm in height and 10,5 cm in diameter as shown in Figure 2. This shape was chosen in order to generate pressure direction like a warhead. A booster on top of the cylinder was used to shelter the primary charge of explosive that was triggered by an electrical fuse. Non-confined explosives have been widely used for blast tests in order to measure blast wave effects (Netherton *et al.*, 2014). The main reason is because records from blast effects are more reliable when there are no explosive fragments. The research team was housed in a bunker by 250 m far from the detonation point while conducting the experiment.

High explosives are standardized by equivalent TNT charges of weight (Draganić & Sigmund, 2012; Koccaz *et al.*, 2008; Li *et al.*, 2016; Zhao & Chen, 2013).
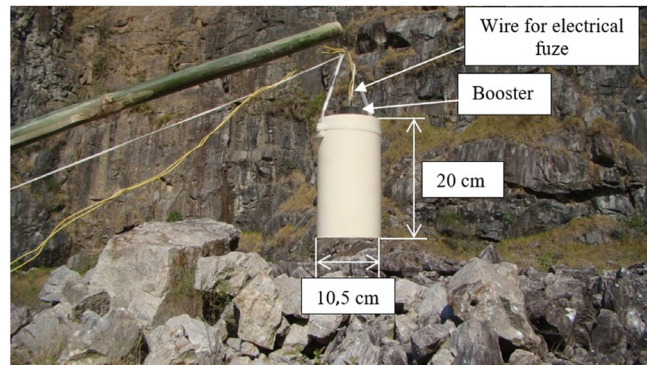

Figure 2. Plastic explosive suspended at the setup before test.
Source: Authors

A scaled distance (Z) is defined by the equivalent TNT mass (W) and stand-off distance (R) as shown in Equation (1) (Brode, 1955; Draganić & Sigmund, 2012; Zhao & Chen, 2013). Table 1 shows the scaled distance values of the four tests.

$$Z = \frac{R}{W^{1/3}} \qquad (1)$$

Table 1. Scaled distance. Values used in the experimental tests

SLABS	W (kg)	R (m)	Z (m/kg$^{1/3}$)	Reinforcement ratio (%)	Foam retrofit
1	2,71	2,0	1,43	0,175 and 0,37	NO
2	2,71	2,0	1,43	0,175 and 0,37	YES
3	2,58	2,0	1,45	0,175 and 0,37	NO
4	2,72	2,0	1,43	0,175 and 0,37	YES

Source: Authors

Explosions near structures, such as the case in the experimental test described in this paper, will experience multiple reflected pressure (PR) (Li *et al.* 2016; Maji *et al.* 2008). Figure 3 shows an example of time-history curve recorded by pressure sensors during the first slab test. It is worth to note that more than one peak of reflected pressure were recorded during the shock wave positive phase. It was due the short scaled distance.
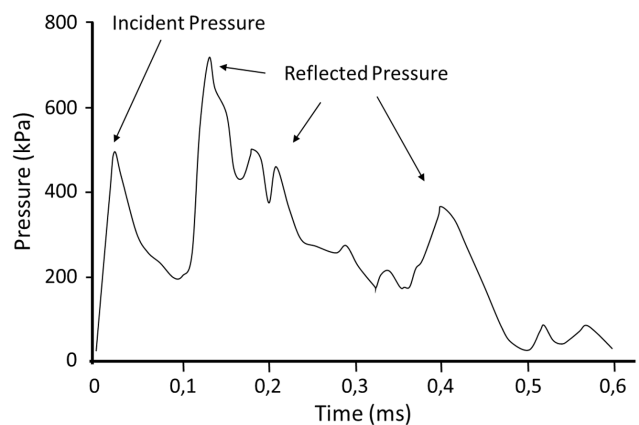

Figure 3. Time-history curve recorded for test of slab 1.
Source: Authors

Integration of the area under the curve of the positive phase of the blast wave results in the specific positive impulse acting on the target (Ngo *et al.*, 2007). Positive impulse is the main parameter that causes damage to structures in blast events (UNODA, 2011). The higher the reflected pressure, the higher the total impulse and it will cause more damage to the target. Multiple peaks of reflection increase the area under the curve and the total impulse as well.

The slabs

Each of the four slabs measured 1,0×1,0×0,08 meters in dimension. The slabs were made with concrete having 50 MPa of static compressive strength. The reinforcing steel had different ratios on the two main perpendicular directions as shown in Figure 4, and it was placed inside the bottom face of the slab to carry positive moment developed due the load direction and boundary conditions.
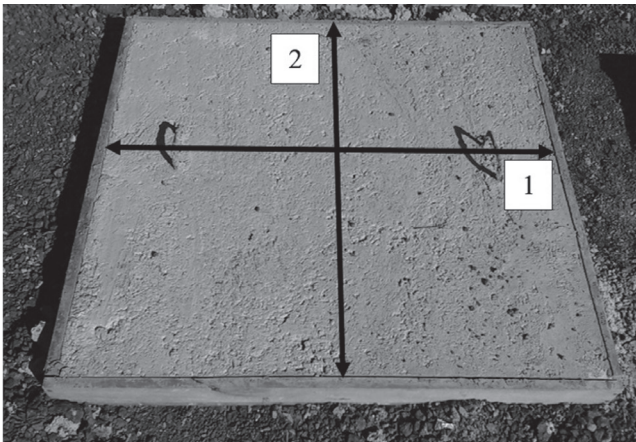

Figure 4. Slab after casting. The main directions are indicated.
Source: Authors

Both directions have 7 reinforcing steel with 5,0 mm in diameter, as shown in Figure 5. However, two more reinforcing steels of 10 mm were added along direction 1 to increase the reinforcement ratio in one direction of the slab, as shown in Figure 6. It was an option to verify the behavior of one more reinforcement ratio.

Figure 5. Reinforcement prepared inside the form before casting.
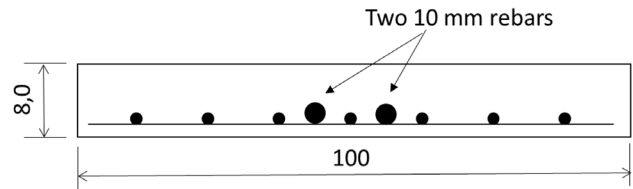**Source:** Authors

Figure 6. Cross-sectional area of the slab in direction 1. Dimensions in cm.
Source: Authors

Equation (2) defines the reinforcement ratio in each direction as the ratio between the area of the reinforcing steel (AS) and the area of the concrete cross-section (AC).

$$\rho_s = \frac{A_s}{A_c} \tag{2}$$

For direction 1, AS was 1,4 cm² and for direction 2 was 2,96 cm². The area of concrete (AC) was 800 cm². Using Equation (2), the reinforcement ratio for direction 1 is 0,175% and for direction 2 is 0,37%.

Two of the four slabs tested had 50 mm of expanded polystyrene foam (EPS) retrofitting on the upper surface (labelled as slab 2 and slab 4 in Table 1), in order to verify if the foam provides reduction of the blast wave effects on the slab response even without thermic protection. Figure 7 shows the EPS applied on top surface of slab 2.
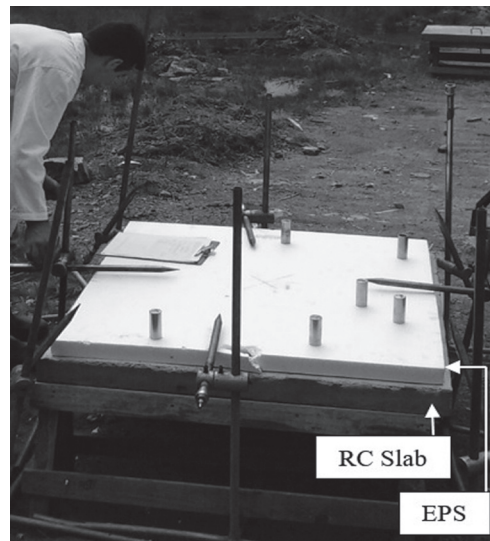

Figure 7. Slab 2 before test with EPS foam on top.
Source: Authors

Instrumentation

Accelerometers were assembled in the Electronic Engineering Laboratory at ITA (Aeronautics Institute of Technology) in DCTA (Science and Technology Aerospace Department). They were made with an Arduino System

consisting of a circuit with 9V DC battery supply, a memory card, and an acceleration sensor MPU 6050. The accelerometers were calibrated using a turntable calibrator to guarantee that their recording was correct. MPU 6050 was attached to the bottom of the slabs to measure the acceleration due the shock wave as shown in Figure 8. The main circuit was placed inside a heavy lead box surrounded internally by foam where it was sheltered from shock wave and debris.

Figure 8. Accelerometer attached to the bottom of the slab before test.
Source: Authors

Two displacement meters were positioned under the bottom surface of the slab inside of a steel box. A tensile wire was fixed on a hook bonded at the center of the bottom surface of the slabs and connected to the displacement sensor. Whilst the slab deflects due to the blast, the wire moves up or down and the displacement sensor records the slab displacement. Figure 9 shows the hooks bonded on the bottom surface of the slab and the steel box where the sensors were sheltered.
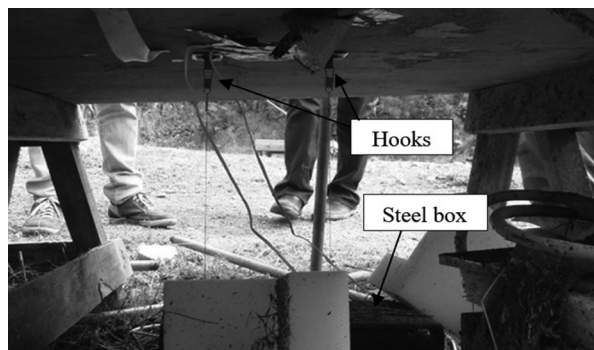

Figure 9. Hooks attached on the bottom of the slab and the steel box sheltering the displacement meter.
Source: Authors

Eight pressure sensors were positioned around the slab at equal distances from the explosive in order to guarantee the same-scaled distance for all tests as shown in Table 1. Four sensors were placed at a higher position to measure incident pressure whereas the remaining sensors were positioned as close to the slab as possible to measure reflected pressure (Figure 1). An Olympus® high-speed digital camera captured still and video images from the explosion event, working with a Toshiba® rugged notebook, recording at 2

500 frames per second (fps). The camera was placed at a distance of 180 m from the explosion.

Results and Discussion

The accelerometer for slab test 1 failed. However, for the remaining three tests it worked well. The acceleration peak during the blast wave action against the slabs can be easily found. The acceleration data for test 2 is shown in Figure 10. The highest peak was 4,36 g (42,77 m/s²) after 0,05 x 10^{-6} s of the trigger.
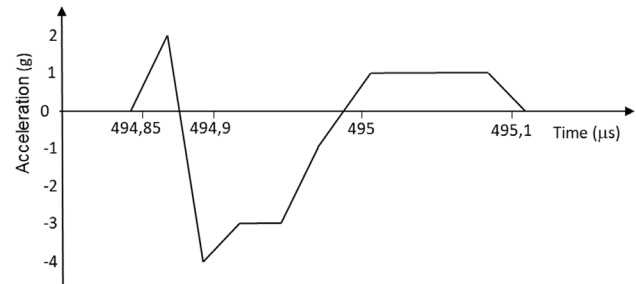

Figure 10. Accelerometer plot for slab 2.
Source: Authors

For Slab 3, the accelerometer recorded a peak of 7,26 g (71,22 m/s²) after 0,024 x 10^{-6} s of the trigger. The recorded data for slab 4 was the highest with the peak of 8,089 g (79,35 m/s²) after 0,024 x 10^{-6} s of the trigger. Further tests are needed to verify accelerometer performance with different values of Z.

Displacement meters were fixed at the center of the bottom surface of the slabs. The displacement meters measured the mid-span deflection of the slabs. Figure 11 shows the displacement-time history recorded for slab 1. This slab did not fail and the peak measured displacement of the slab was 39,8 mm. The drop in displacement and the back up before stabilizing was because of the boundary conditions. The slabs retrofitted with the EPS foam (slabs 2 and 4) experienced a higher linear momentum and they failed. Therefore, the recorded displacement values were not reliable for slab 2 and slab 4. Slab 2 result is included for the sake of completion as shown in Figure 12.

Slab 3 developed minor cracks but did not fail completely with a measured peak displacement of 24,6 mm. Figure 13 shows the displacement-time history data for this slab.

Integration of the displacement-time history of the slabs gives the velocity imparted during the action of the shock wave. The linear momentum developed in the slabs can be calculated once the velocity is determined. Table 2 shows the linear momentum developed in the four tests.
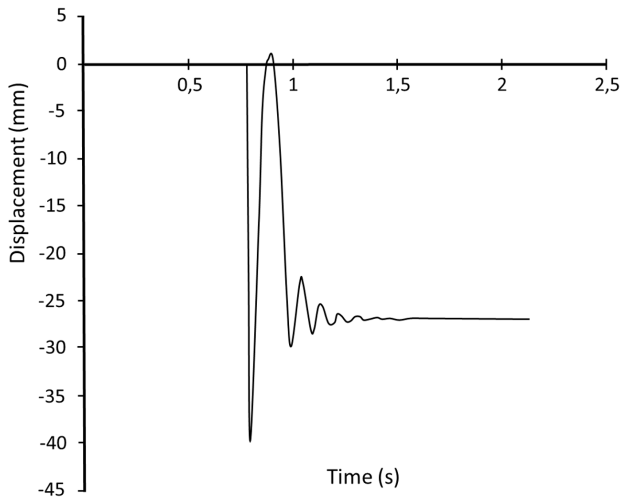
Figure 11. Displacement-time history for slab 1.
Source: Authors

Table 2. Comparison of developed linear momentum

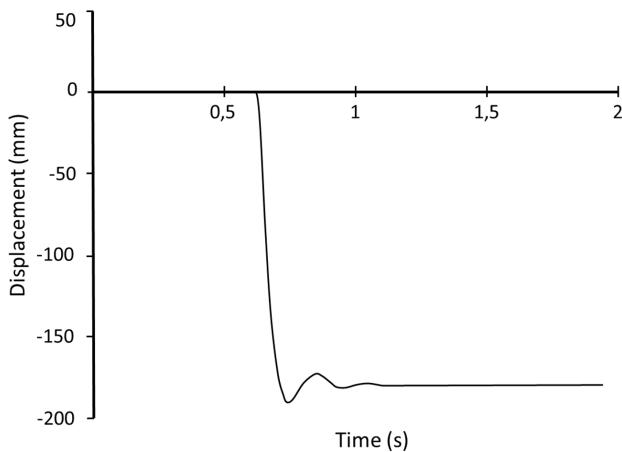| SLABS	Displacement peak (mm)	Time elapsed (ms)	Velocity (m/s)	Mass (kg)	Linear momentum (kg m/s)
1	39,8	27,1	1,46	180	264
2	188,8	130,0	1,45	180	261
3	24,6	44,6	0,55	175	96
4	212,4	85,0	2,49	175	436

Source: Authors

Figure 12. Displacement-time history for slab 2.
Source: Authors

Overalls slabs with EPS foam retrofitting experienced a higher linear momentum when compared to slabs without the foam retrofit. Slab 4 with EPS foam retrofitting developed the highest value of linear momentum, showing that the foam without thermic protection can increase the movement of the element retrofitted while the blast wave shocks the system. Slab 1 did not fail. Slab 2 failed as shown in Figure 14. Slab 3 developed the smallest linear momentum and did not fail as shown in Figure 15.

The piezoelectric pressure sensors recorded blast pressure-time history for all tests. Figure 16 shows the comparison of recorded to theoretical values of incident (Pso) and reflected (Pr) pressure given by the widely used Kingery and Bulmash curves (Kingery & Bulmash, 1984; Swisdak Jr, 1994). Recorded incident pressure was given by the results of sensors at the higher position. Sensors close to the slab gave reflected pressure. The difference between theoretical and recorded incident pressures was 7% for slabs 1 and 2, and 12 % for slabs 3 and 4.
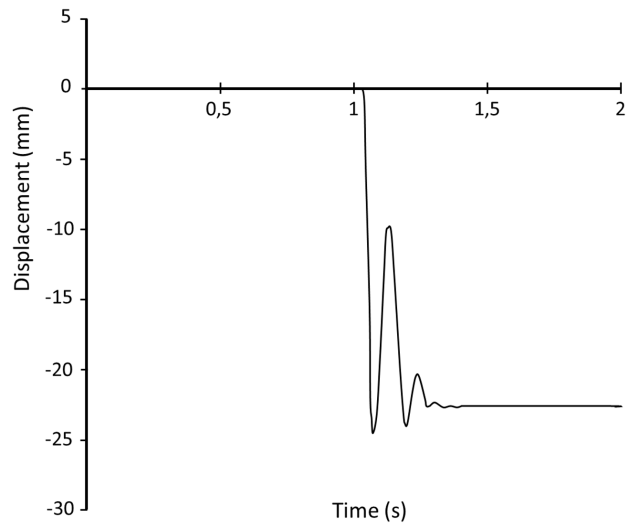

Figure 13. Displacement-time history for slab 3.
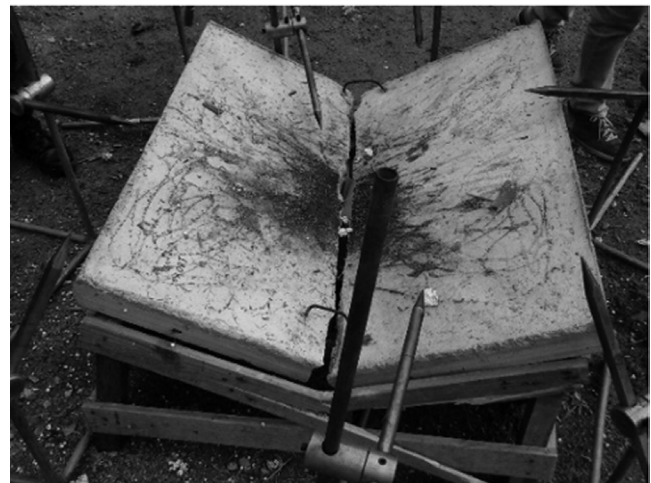**Source:** Authors

Figure 14. Slab 2 after test.
Source: Authors

Theoretical value of reflected pressure was given by Kingery and Bulmash curves (Kingery & Bulmash, 1984; Swisdak Jr, 1994) as well. Slabs 2 and 4 showed the highest difference from theoretical predicted values, having predicted values 35% and 38% higher than the recorded respectively. Slab 1 had recorded value 6% higher than predicted value and for slab 3 the predicted value was 7% higher than recorded. We attribute these differences because of uncertainties

involved in the physical system due to the small-standoff distances of the explosions.

Figure 15. Slab 3 after test.
Source: Authors

As the slabs had different reinforcement in mutually perpendicular direction, it was possible to verify that the collapse happened in the direction with lower reinforcing steel. The slabs with EPS foam without thermic isolation (slab 2 and slab 4) could not support the blast pressure and failed as shown in Figure 15. However, reflected pressure for slabs with foam was 40% lower in average. Post-video analysis revealed that the EPS foam burned during the detonation as shown in Figure 17.
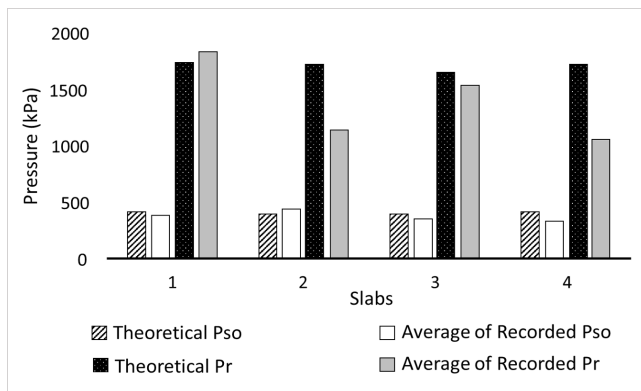

Figure 16. Comparison of theoretical and average of recorded incident and reflected pressures.
Source: Authors

Slabs 1 and 3 (Figure 15) resisted the blast effect in a better way than slabs having EPS foam retrofits. These slabs did not fail and remained in the original position even if they developed some cracks. The main and radial cracks generated at the bottom surface can be clearly seen in Figure 18.

Reflected pressure can increase specific positive impulse. Due to this, impulse is the effect that brings damage to the slab in these tests.

Tests with larger slabs are being planned to confirm the response of a real size reinforced concrete slab.

Figure 17. Explosion of slab 2. The circle highlights the EPS being burned. Image recorded 9,6 m after trigger.
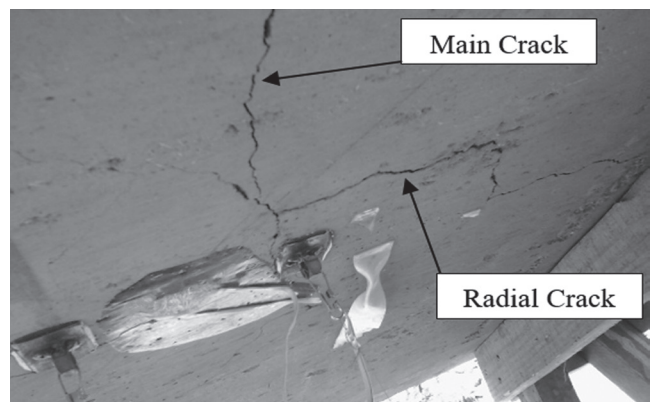**Source:** Authors

Figure 18. Post-test of slab 1. View of the bottom face.
Source: Authors

Conclusions

Four reinforced concrete slabs having 50 MPa compressive strength and 0,175% reinforcement ratio in one direction and 0,37% in the perpendicular direction were subjected to blast effect of non-confined PBX explosive. The explosive was suspended at a stand-off distance of 2,0 m and had the same scaled distance for the four tests. The equation used for the comparison of theoretical and recorded values for blast pressure worked well within 7-12% for incident and reflected pressures. Two of the four slabs had EPS foam retrofit in order to investigate whether the foam helps absorb the blast energy or not. It was observed that EPS foam without thermic protection did not help resist the blast load, instead exacerbated the response by generating a higher linear momentum. This observation agrees with Lee and O'Toole research (2004) that shows the possibility of the foam retrofitted having an unwanted consequence in resisting blast loads. The slabs without foam retrofitting resisted the effects of the shock wave without collapse following a sound engineering design of reinforcing steel.

References

Brode, H. L. (1955). Numerical solutions of spherical blast waves. *Journal of Applied Physics*, *26*(6), 766–775.

Castedo, R., Segarra, P., Alañon, A., Lopez, L. M., Santos, A. P., & Sanchidrian, J. A. (2015). Air blast resistance of full-scale slabs with different compositions: Numerical modeling and field validation. *International Journal of Impact Engineering*, *86*, 145–156. http://doi.org/10.1016/j.ijimpeng.2015.08.004

Draganić, H., & Sigmund, V. (2012). Blast loading on structures. *Tehnički Vjesnik*, *19*(3), 643–652.

Kingery, C. N., & Bulmash, G. (1984). *Airblast Parameters From TNT Spherical Air Bursts and Hemispherical Surface Bursts*. Maryland.

Kirchhof, E., Rocha, R. J., Nakamura, N. M., Lapa, C. M., Pinheiro, G. F. M., Gonçalves, R. F. B., … Iha, K. (2016). Estimativa de vida útil do PBX (plastic-bonded explosive) com envelhecimento acelerado. *Química Nova*, *39*(6), 661–668. http://doi.org/http://dx.doi.org/10.5935/0100-4042.20160072

Koccaz, Z., Sutcu, F., & Torunbalci, N. (2008, October). Architectural and Structural Design for Blast Resistant Buildings. In *The 14th World Conference on Earthquake Engineering*. Beijing.

Lee, D. K., & O'Toole, B. J. (2004, May). Energy absorbing sandwich structures under blast loading. *8th International LS-DYNA Users Conference*, 13–24. Dearborn, MI. https://www.dynalook.com/international-conf-2004/08-2.pdf

Li, J., Wu, C., Hao, H., Wang, Z., & Su, Y. (2016). Experimental investigation of ultra-high performance concrete slabs under contact explosions. *International Journal of Impact Engineering*, *93*, 62–75. http://doi.org/10.1016/j.ijimpeng.2016.02.007

Maji, A. K., Brown, J. P., & Urgessa, G. S. (2008). Full-Scale Testing and Analysis for Blast-Resistant Design. *Journal of Aerospace Engineering*, *21*(4), 217–225. http://doi.org/10.1061/(ASCE)0893-1321(2008)21:4(217)

Mendonça, F. B., Urgessa, G. S., & Rocco, J. A. F. F. (2017, april). Blast Response of 60 MPa Reinforced Concrete Slabs Subjected to Non-Confined Plastic Explosives. In *Proceeding of 2017 Structures Congress, American Society of Civil Engineers*, 15–26. Denver, CO, http://ascelibrary.org/doi/10.1061/9780784480397.002

Mullin, M. J., & O'Toole, B. J. (2004, May). Simulation of Energy Absorbing Materials in Blast Loaded Structures. *8th International LS-DYNA Users Conference*, 67–80. Dearborn, MI.

Netherton, M., Stewart, M. G., Buttenshaw, S. J., Reidy, K., & Rodgers, B. A. H. (2014). *Experimental Data from The University of Newcastle's July 2014 Repeatable Explosive Field Trials*. New South Wales.

Ngo, T., Mendis, P., Gupta, A., & Ramsay, J. (2007). Blast loading and blast effects on structures - An overview. *Electronic Journal of Structural Engineering*, *7*, 76–91.

Petel, O. E., Ouellet, S., Higgins, A. J., & Frost, D. L. (2013). The elastic-plastic behaviour of foam under shock loading. *Shock Waves*, *23*(1), 55–67. http://doi.org/10.1007/s00193-012-0414-7

Swisdak Jr, M. M. (1994). *Simplified Kingery Airblast Calculations*. Arlington: Naval Surface Warfere Center.

UNODA. (2011). *International Ammunition Technical Guideline (United Nations SaferGuard)* (2nd ed.). New York.

Urgessa, G., & Maji, A. (2010). Dynamic Response of Retrofitted Masonry Walls for Blast Loading. *Journal of Engineering Mechanics-Asce*, *136*(7), 858–864. http://doi.org/Doi 10.1061/(Asce)Em.1943-7889.0000128

Zhao, C. F., & Chen, J. Y. (2013). Damage mechanism and mode of square reinforced concrete slab subjected to blast loading. *Theoretical and Applied Fracture Mechanics*, *63–64*, 54–62. http://doi.org/10.1016/j.tafmec.2013.03.006